International Scientific Colloquium
Modelling for Saving Resources
Riga, May 17-18, 2001

Adiabatic Steam Stripping of PAH Contaminated Droplets in Reactor Tube

A. Jakovics, V. Frishfelds, J. Hoehne, B. Niemeyer, A. Eschenbach

Abstract

The process of steam stripping of two-component sludge is described in isobaric approximation. The phase diagram of PAH-water is constructed using the linear dependence of partial pressure of component on its molar fraction outside the miscibility gap. The process is split in two stages: relatively fast diffusion controlled saturation of the partial pressures and heat transfer controlled evaporation.

Introduction

Soils contaminated by PAH (polycyclic aromatic hydrocarbons) are extremely hazardous to living organisms. GKSS research centre has developed and built up a pilot equipment to clean soil polluted with PAH by steam stripping. The average size of previously refined soil particles in experiments lies between 10 and 100 μm. Before treatment, the contaminated soil is mixed up with water forming a sludge. This mixture is pushed into the reactor tube through a nozzle using a stream of hot water vapour (see Fig. 1). The PAH are transferred from the sludge to the gaseous steam phase during the steam stripping process. By means of the nozzle and the strong turbulent conditions at the outlet of the nozzle, overheated stem is mixed up with sludge droplets. Therefore, let us consider small sub-system (cell) of the resulting mixture that consists of one droplet and vapour around it. The mass ratio of the droplet and vapour equals to their supply ≈1/10. This ratio and initial steam temperature up to 400 °C is enough for evaporating all of the water in the sludge. The steam stripping in the cell can be assumed as nearly adiabatic as the heat exchange between the cell and reactor walls is neglectable in such a short interval of time needed for the process.

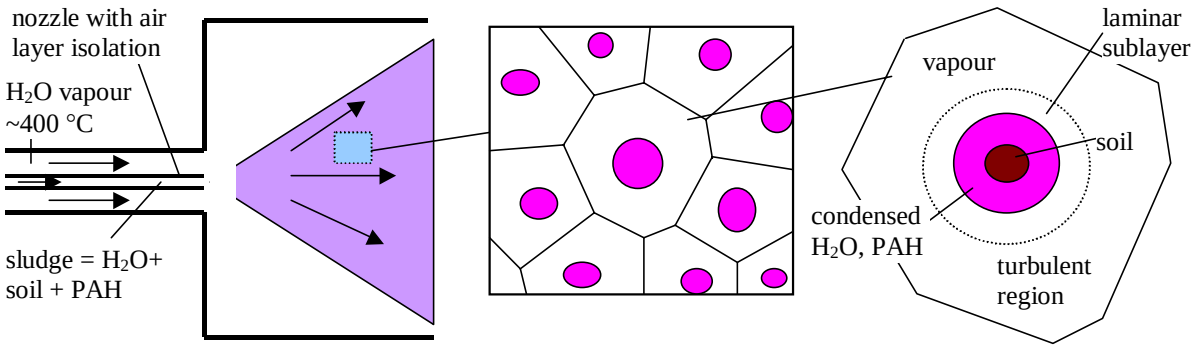

Fig. 1. Spraying of the sludge added by superheated steam and steam stripping of PAH contaminated droplets

1. Construction of PAH-Water Phase Diagram

The liquid part of the sludge and vapour consists of two components: water and PAH. One characteristic feature of such a PAH-water system is an extremely small solubility of one component into another. Thus, there exists a huge miscibility gap [1]. Consequently, the pressure of the system is independent of the PAH fraction inside the miscibility gap. This is shown in the *P-x* phase diagram of Fig. 2 by a plateau. If the fraction of a given component is smaller than its solubility, its pressure it is approximately proportional to its molar fraction. The deviations from this rule can be considered in further calculations. The linear approximation means that activity coefficient does not depend on molar fraction in this range. Thus activity coefficient is the reciprocal of molar solubility [2]. At the opposite side of phase diagram the pressure increases slightly,- it must tend to Raoult's law at the end. However, the both solubilities are so small that there is really no influence of it. The total pressure of the system is given by the sum of partial pressures of related component. There is no chemical reaction assumed between water and PAH. Molar solubility follow approximately to Henry's law:

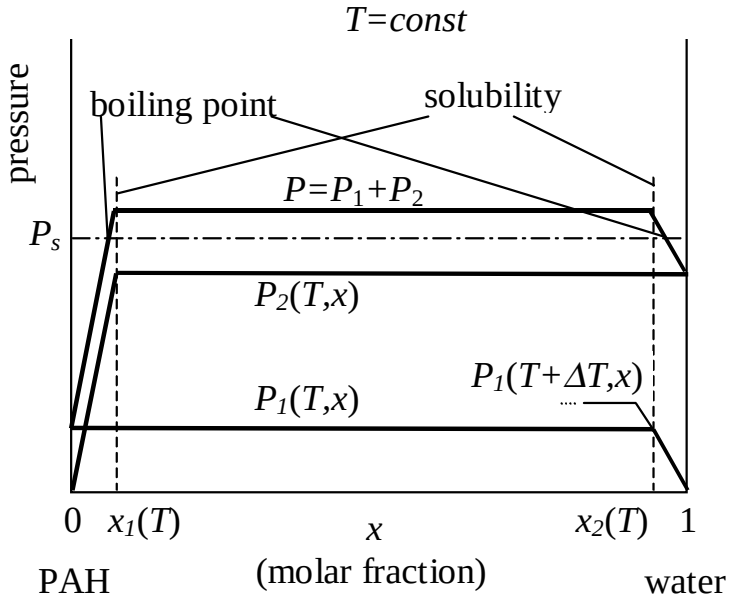

Fig. 2. Partial pressures of the components

$$S(T) = k_H(T)P(T), \tag{1}$$

where $P(T)$ is pressure of the component. Let us consider, that Henry's constant k_H in our case is nearly independent on temperature. That is of course a rough approximation as it could increase for PAH in water by an order of magnitude from 298 K to 373 K [3]. The consequence of Henry's law is that the slope of the partial pressure outside miscibility gap (see Fig. 2) does not change increasing the temperature. Thus, we should now the solubility only at one temperature say at azeotrope T_e. The temperature of the azeotrope T_e, which for the PAH-water system is very close to boiling temperature of water, can be determined from Dalton's law

$$P_1(T_e) + P_2(T_e) = P_s, \tag{2}$$

where P_s is the pressure of the system, $P_1(T)$, $P_2(T)$ are the partial pressures of PAH and water at plateau, respectively. In our case, the partial pressure at plateau equals to pressure of pure component under the same temperature conditions. The Antoine data for pressure are readily available for:

$$\ln P(T) = A - \frac{B}{T + C} \tag{3}$$

with some constants *A, B, C*. An approximation of liquid-vapour data by more complicated formulas, e.g. [4], is useful in broader range of temperatures, but they are worse in particular range of temperatures as in our case. Solubilities $x_1(T)$, $1\text{-}x_2(T)$ follow from (1):

$$x_1(T) = x_1(T_e)\frac{P_2(T)}{P_2(T_e)}, \quad 1 - x_2(T) = (1 - x_2(T_e))\frac{P_1(T)}{P_1(T_e)}. \tag{4}$$

The boiling points corresponds to the points where pressure of the system P_s crosses the sum P in Fig. 2

$$x_{b1}(T) = x_1(T)\frac{P_s - P_1(T)}{P_2(T)}, \qquad 1 - x_{b2}(T) = (1 - x_2(T))\frac{P_s - P_2(T)}{P_1(T)}. \tag{5}$$

Applying the Dalton's law again, dew-points are

$$x_{d1}(T) = \frac{P_2(T)}{P_s}, \qquad 1 - x_{d2}(T) = \frac{P_1(T)}{P_s}. \tag{6}$$

This equation gives also molar fraction of azeotropic mixture x_e at $T = T_e$. The constructed phase diagram of naphthalene-water by the formulas above is shown in Fig. 3 at various scales.

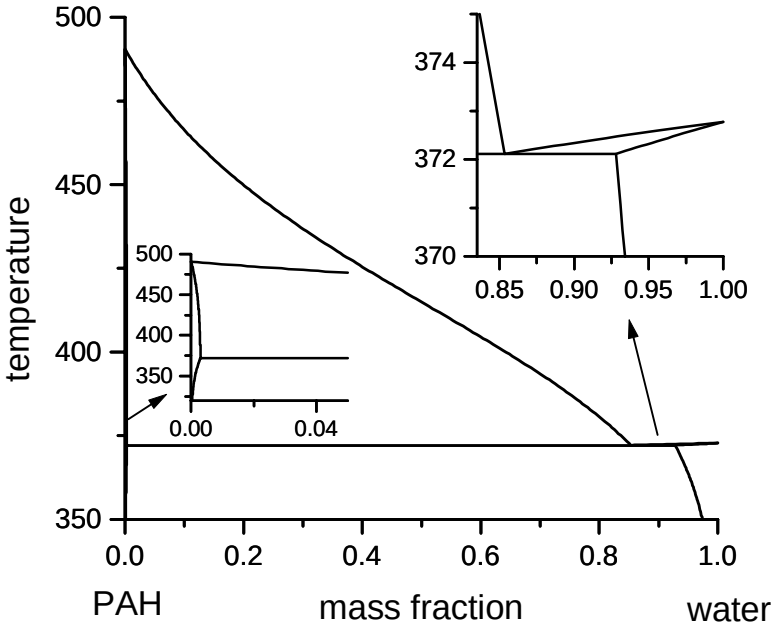

Fig. 3. Constructed phase diagram of naphthalene-water

2. Dynamics of Isobaric Steam Stripping

The shape for the droplet should be nearly spherical with soil particle placed at the centre. The coefficient of heat conductivity in condensed material usually is higher than in gases. Therefore, the temperature difference inside the small droplet with diameter ≈100 μm, of course, is ever smaller than in the steam phase while the diameter of the cell is about 3 mm. That could be said also about the concentration of PAH, if the PAH phase is present on the surface of the droplet. The evaporation process predominantly should be heat transfer controlled as $q >> \frac{i}{2}kT$ with q - heat of evaporation per one molecule, $i = 5 \div 6$ - degrees of freedom, k – Boltzmann constant. Therefore the distribution of PAH and water in vapour phase is almost homogeneous.

Let us separate the process in two stages. The saturation of partial component pressures in vapour phase and sludge appears in the first stage of the process which takes place in very small time compared to the second one. Therefore, the absolute values of diffusion coefficients are less important. At the second stage the binary mixture is evaporating due to heat transfer towards droplet. This process is heat transfer controlled and follows to the phase diagram.

2.1. Saturation of Partial Pressures

The average velocity of molecules in gas is inversely proportional to the square root of their molar mass. On other hand, the mean free path is inversely proportional to the square of the size of molecule. Hence, the ratio of diffusion coefficients of PAH and water in steam is

$$\frac{D_1}{D_2} \approx \sqrt{\frac{\mu_2}{\mu_1}}\left(\frac{\rho_1\mu_2}{\rho_2\mu_1}\right)^{2/3}, \tag{7}$$

where μ is molar mass, ρ - density in condensed phase, indexes: 1 - PAH, 2 - water. Steam initially contains no PAH. Hence, PAH transfers from sludge to vapour. At the same time, the water pressure in the vapour phase is higher than that of the droplet as the initial temperature is kept lower than the temperature of azeotrope. The molar amount of components M_1, M_2 changes according to

$$\frac{\partial M_1}{\partial t} \sim D_1\left(P_s(1-y) - P_1(T,x)\right), \qquad \frac{\partial M_2}{\partial t} \sim D_2\left(P_s y - P_2(T,x)\right), \tag{8}$$

where x, y are the molar fraction of water in droplet and vapour, respectively. Effects of surface tension are unimportant for the sizes of the droplet above micrometer scale. Due to condensation of water and evaporation of PAH some heat is created:

$$\Delta Q_q = q_1(T,x)\mu_1\Delta M_1 + q_2(T,x)\mu_2\Delta M_2, \tag{9}$$

where $q_1(T,x)$, $q_2(T,x)$ are heat of evaporation per one mole of the respective component. This heat, furthermore, changes the temperature of the droplet:

$$\Delta Q_c = (C_{p1}(T)M_1 + C_{p2}(T)M_2 + c_s m_s)\Delta T, \tag{10}$$

where $C_{p1}(T)$, $C_{p2}(T)$ are molar heat capacities of components; c_s, m_s are heat capacity and mass of soil particle inside the droplet. The heat of evaporation is related to saturation pressure by Clausius-Clapeyron law:

$$q(T) = \frac{\partial P}{\partial T}T\left(\frac{1}{\rho_g(T)} - \frac{1}{\rho_l}\right), \tag{11}$$

where ρ_g, ρ_l are densities in gas and liquid phase, respectively. The constructions in Fig. 2 show that heats of evaporation are

$$q_1(T,x) = \begin{cases} q_1(T), & x \le x_2(T) \\ 0, & x > x_2(T) \end{cases}, \; q_2(T,x) = \begin{cases} q_2(T), & x \ge x_1(T) \\ 0, & x < x_1(T) \end{cases}, \tag{12}$$

where $q_1(T)$, $q_2(T)$ are heat of evaporation of pure components. The characteristic scenario of diffusion is shown in Fig. 4. One can split the process again in two subparts due to slow much slower diffusion of PAH (7) in the steam, i.e., water pressure saturates first, and PAH evaporates afterwards relatively slowly. As can be seen, the droplet curve ends at boiling point and vapour line at dew point. That acts as the initial condition for the second stage of the process described below. This position lies on the same side of phase diagram with respect to azeotropic mixture x_e as the fraction of water in all PAH-water cell x_t does. The position of x_t is shown by dot-dashed line in Fig. 4. For example, for naphthalene in Fig. 4 diffusion ends at the right side of the azeotrope, while for pyrene in Fig. 5 – at the opposite one.

2.2. Heat Transfer Controlled Evaporation

The second stage of the process takes place so that the water fraction in droplet coincides with boiling curve, while fraction in vapour with dew one. It can be easily simulated by equalisation of the right hand side of (8) with zero. The evaporation finishes when dew curve crosses with total fraction x_t, when all the mixture is evaporated. That can be seen in enlarged scale of Fig. 4 by small increase of temperature after the end of the first stage.

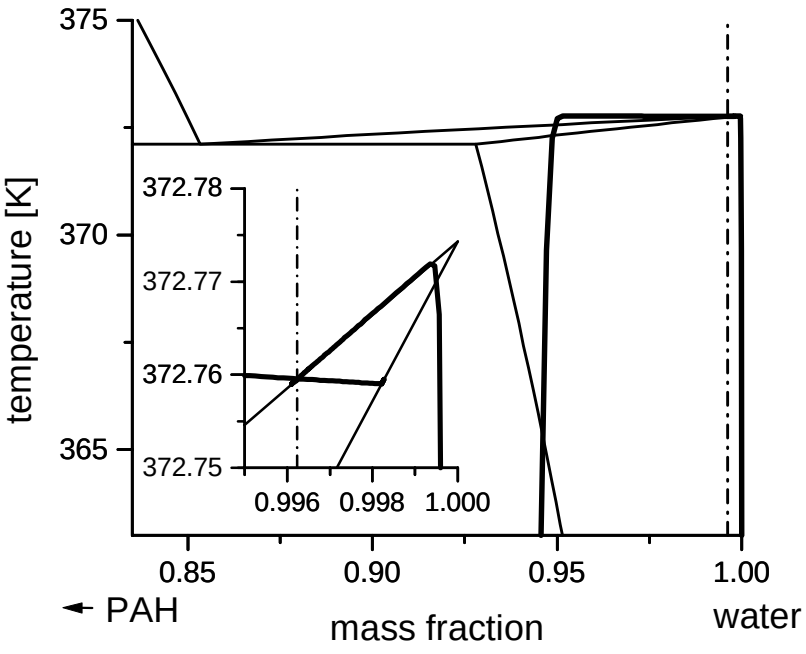

Fig. 4. Dynamics of the stripping in phase diagram, Fig. 3. Thick curves correspond to droplet and vapour at surface temperature. Dot-dashed line – total mass fraction x_t in cell

If the steam fraction and its temperature is insufficient, the process stops when the temperatures of steam and droplet equalises. The radiation heat transfer is unimportant for characteristic temperatures in reactor and sizes of droplets below millimetre. The use of Stokes law show that initial average velocity difference between steam and vapour decreases faster than evaporation of sludge. However, there exists some local stochastic difference of velocities, and the heat and mass transfer between vapour and droplet is turbulent like that increases the heat transfer to the droplet. The coefficient of heat transfer is approximately proportional to the temperature difference. The proportionality coefficient can be interpreted by some effective thickness of relatively thin laminar sublayer around the droplet and other part, where high turbulence takes place. The temperature and concentration in the turbulent region is almost constant. Heat transfer from steam to droplet

$$\frac{\partial Q_\lambda}{\partial t} = \frac{4\pi}{\frac{1}{r} - \frac{1}{r+\delta_{lam}}} \int_T^{T_v} \lambda(T) dT \,, \tag{13}$$

must be added in (10), where r is the radius of the droplet, δ_{lam} – thickness of laminar sublayer, $\lambda(T)$ – coefficient of heat conductivity in steam, T_v vapour temperature in turbulent region. This heat transfer causes the cooling of vapour

$$\Delta Q_\lambda = -\left(\frac{i_1 + 2}{2} M_{1v} + \frac{i_2 + 2}{2} M_{2v} \right) R \Delta T_v \,, \tag{14}$$

where R is universal gas constant; i_1, i_2 – degrees of freedom; M_{1v}, M_{2v} – molar amount of components in vapour phase.

The degree of PAH cleaning, temperatures and radius of the droplet during steam stripping of pyrene-water system are shown on Fig. 5. The time scale of diffusion controlled approach here is chosen arbitrarily. The size of the droplet increases in first stage of the process but decreases more rapidly in next stage reaching the size of the soil particle. As the total fraction of water is lower than of azeotrope, the water fraction in droplet decreases up to the moment when the solubility limit of water in pyrene is reached. Afterwards, strong evaporation of pyrene and increase of the temperature of the droplet takes place.

The total size of the cell in Fig. 1 decreases by approximately 3 % in the described isobaric evaporation. However, the pressure would remain constant only if the scattering angle in Fig. 1 is close to zero. In general, the pressure of the system decreases behind the opening of the pipe as the vapour-sludge mixture diffracts. The temperature would remain approximately constant for laminar diffraction of ideal gas. Thus, the non-monotonous decreases of remained PAH content in droplet is possible. However, that spoils the understanding of the process while the qualitative behaviour of the process does not change.

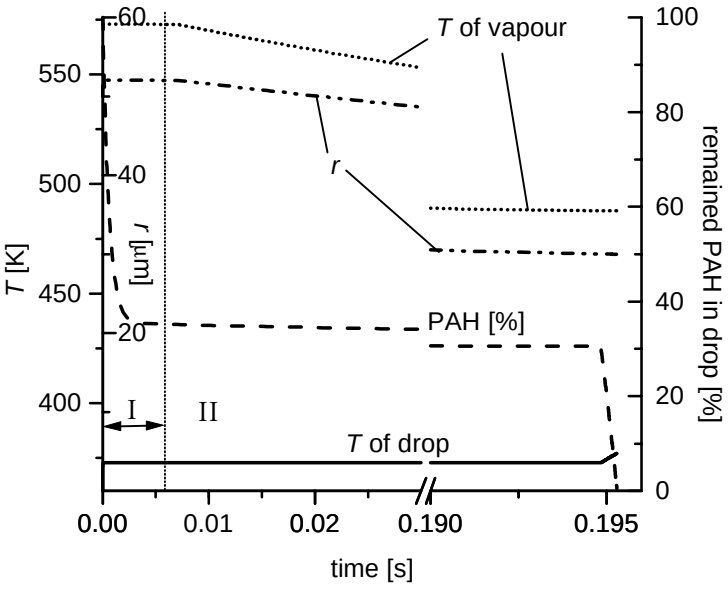

Fig. 4. Behaviour of the temperature of droplet and vapour, radius of droplet, and amount of PAH remained in the drop at steam stripping of pyrene. I – diffusion controlled approach, II – heat transfer controlled approach

Conclusions

The phase diagram of chemically non-interacting components can be constructed using the properties of pure components and dependence of partial pressures on the constitution of the binary mixture.

The saturation of pressures finishes at the same side in phase diagram with respect to azeotropic fraction as total fraction of the system does.

The size of the system decreases at isobaric conditions despite of evaporation of the droplet.

References

[1] Kirschbaum, E.: *Destilier un Rektifiziertechnik*. Springer-Verlag, Berlin, 1969.

[2] Hwang Y.-L., Olson, J.D., Keller, G.E: *Steam stripping for removal of organic pollutants from water. 2. Vapor-liquid equilibrium data*. Ind. Eng. Chem. Res. Vol. 31, 1992, pp. 1759-1768.

[3] Ten Hulscher, Th.E.M., van der Velde, L.E., Bruggeman, W.A.: Temperature dependence of Henry's law constants for selected chlorobenzenes, polychlorinated biphenyls and polycyclic aromatic hydrocarbons. Environmental Toxicology and Chemistry, Vol. 11, 1992, pp. 1595-1603.

[4] Yaws, C. L.: *Chemical properties handbook*. McGraw-Hill, New York, 1999.

Authors

Dr.-Phys. Jakovics, Andris
E-mail: ajakov@latnet.lv
Dipl.-Phys. Frishfelds, Vilnis
E-mail: mf60006@lanet.lv
Faculty of Physics and Mathematics
University of Latvia
Zellu 8, LV-1002 Riga, Latvia

Dr.-Ing. Hoehne, Joachim
E-mail: hoehne@gkss.de
Prof. Dr.-Ing. Niemeyer, Bernd
E-mail: niemeyer@gkss.de
Dr.-Nat. Eschenbach, Annette
E-mail: eschenbach@gkss.de
GKSS-Forschungszentrum GmbH
Max-Planck-Straße, 21502 Geesthacht, Germany